AIP | Journal of Applied Physics

Ferromagnetic resonance study of FeCoMoB microwires during devitrification process

P. Klein, R. Varga, G. Infante, and M. Vázquez

Citation: J. Appl. Phys. **111**, 053920 (2012); doi: 10.1063/1.3689789

View online: http://dx.doi.org/10.1063/1.3689789

View Table of Contents: http://jap.aip.org/resource/1/JAPIAU/v111/i5

Published by the American Institute of Physics.

Ferromagnetic resonance study of FeCoMoB microwires during devitrification process

P. Klein,[1] R. Varga,[1,a)] G. Infante,[2] and M. Vázquez[2]
[1]*Institute of Physics, Faculty of Sciences, P. J. Safarik University, Park Angelinum 9, 041 54 Kosice, Slovakia*
[2]*Instituto de Ciencia de Materiales de Madrid, CSIC, 28049 Madrid, Spain*

(Received 4 March 2011; accepted 1 February 2012; published online 8 March 2012)

Magnetic properties of FeCoMoB glass-coated microwires with high positive magnetostriction have been investigated during the process of devitrification in the temperature range: 0-600 °C by ferromagnetic resonance (FMR) studies. The FeCoMoB microwire shows natural ferromagnetic resonance that reflects a complex anisotropy distribution. FMR spectrum for as cast sample shows up to four resonance maxima when ranging frequency from 10 MHz up to 11.3 GHz. After annealing, the anisotropy distribution becomes more regular and the number of FMR peaks decreases. The anisotropy and stress amplitude has been estimated from the FMR spectra, showing a strong decrease with annealing temperature and being low and constant for the nanocrystalline state. In addition, Gilbert damping decreases with annealing temperature, too. The low Gilbert damping (~0.01) for the nanocrystalline state makes the nanocrystalline FeCoMoB microwire an ideal material for applications in which fast magnetization processes are required. © *2012 American Institute of Physics*. [http://dx.doi.org/10.1063/1.3689789]

I. INTRODUCTION

Amorphous glass-coated microwires are magnetic systems that are attracting recently much interest from the fundamental magnetism studies as well as from the applications point of view.[1–4] For example, microwires exhibiting negative or nearly zero magnetostriction are very suitable as sensing elements in devices based on the giant magnetoimpedance effect. In turn, microwires with high positive magnetostriction present magnetic bistability, which is applicable in many modern microsensors devices. Glass-coated microwires offer some important advantages in comparison with their ribbon counterpart as: small dimensions and symmetrical shape, less-expensive preparation and reliability on electrical, mechanical, and enhanced corrosion resistance from Pyrex coating. These microwires are produced by quenching and drawing technique, during which strong mechanical stresses are introduced. It was shown that axial stresses prevail in a central core of the wire, while radial stresses are dominant just below the surface.[5] Due to their amorphous structure the magnetic properties of amorphous microwires are thus controlled by magnetoelastic and shape (magnetostatic) anisotropies. As a result, the domain structure in microwires with positive magnetostriction is characterized by a large internal single domain with axial magnetization that is surrounded by a radial multi-domain structure. Moreover, small closure domains appear at the ends of the wire to reduce the stray fields. Such a domain structure results in the magnetization process that is characterized by a single Barkhausen jump due to the propagation of a wall from the closure structure that is characteristic for magnetic materials showing bistability.

On the other hand, nanocrystalline magnetic materials exhibit excellent magnetic properties as high thermal and structural stability, quite low coercivity, high saturation magnetization, high initial permeability, low core loss, and relatively high resistivity.[6–8] The influence of nanocrystallization process on magnetic bistable behavior has been thoroughly studied both on FeSiBCuNb (FINEMET) wires and microwires.[9–11] On the other hand, nanocrystalline FeCoMoB microwires based on HITPERM composition have particularly more elevated Curie temperature and larger saturation magnetization at very high temperatures in comparison with FINEMET based nanocrystalline microwires.[12–14] In addition, FeCo based alloys,[15] and in particular FeCoMoB microwires, have outstanding soft magnetic properties after thermal treatment at optimal annealing temperature within a wide temperature range (450-600 °C).[16] These microwires exhibit bistability even in advanced nanocrystalline state. Further detailed information about studied nanocrystalline FeCoMoB microwires can be found elsewhere.[16]

Ferromagnetic resonance measurements is a simple, sensitive, powerful, and very suitable tool to determine in a ready manner intrinsic magnetic parameters such as saturation magnetization, anisotropy field, Gilbert damping, or Landé factor as well as the presence of magnetic inhomogeneities, internal stresses, or the skin effect penetration depth.[17–21] Ferromagnetic resonance experiments have also reported on nanocrystalline FeCo-based alloys[22] and particularly in nanocrystalline microwires.[23,24] A suitable method to study of ferromagnetic resonance in magnetic wires is based on magnetoimpedance measurements.[14] It was shown that high frequency impedance measurements in ferromagnetic wires under a longitudinal magnetic field fit perfectly an electromagnetic-field geometry configuration as required for ferromagnetic resonance (FMR).[25,26] In the particular case when $M_s >> (H_0 + H_k)$, where M_s denotes the saturation magnetization, H_0 the longitudinal applied field and $H_k = 2K/\mu_0 M_s$ the anisotropy field, the evolution of resonance frequency with static axial field H_0 can be approximated as[1]

a)Author to whom correspondence should be addressed. Institute of Physics, Faculty of Sciences, UPJS Park Angelinum 9, 041 54 Kosice, Slovakia. Electronic mail: rvarga@upjs.sk.

$$f_r = \frac{\gamma\mu_0}{2\pi}\sqrt{M_S(H_0 + H_k)}, \quad (1)$$

where γ is the gyromagnetic ratio, μ_0 is the vacuum permeability.

The aim of this paper is to investigate the evolution of magnetic properties in FeCoMoB microwire during its devitrification, starting from initial amorphous state up to advanced nanocrystalline state. It is shown that stable nanocrystalline microstructure leads to the lower stress amplitude and lower anisotropy in the FeCoMoB microwires. Studied amorphous and nanocrystalline FeCoMoB microwires exhibit strong natural ferromagnetic resonance observed in the absence of applied static magnetic field. Furthermore, the evolution of anisotropy field, Gilbert damping (the parameter reflecting the damping of individual magnetic moments during their precession[27]) and internal stresses with increasing annealing temperature is shown.

II. EXPERIMENTAL TECHNIQUES

Amorphous glass-coated microwires with $Fe_{40}Co_{38}Mo_4B_{18}$ nominal composition were produced by the Taylor-Ulitovsky method. The diameter of the metal core was 16 μm and the thickness of the glass coating 9 μm. These microwires were annealed for 1 h under an argon atmosphere at different temperatures ranging from 200 °C up to 600 °C. Three characteristic samples, in a similar way as previously performed by other authors in the case of amorphous wires,[11] were selected to show the effect of the structure on the FMR measurements: i) as-cast sample with high and complex stress distribution, ii) sample annealed at 400 °C—the temperature at which stress relaxation and homogenization of amorphous nucleus is already completed, and iii) sample annealed at 450 °C, when the metallic nucleus appears in nanocrystalline state.[16]

The length of all samples used in ferromagnetic measurements was 8 mm. The ferromagnetic resonance FMR has been studied with an Agilent PNA E8362B network analyzer in the range of frequency from 10 MHz up to 11.3 GHz at a constant power of 0 dBm (=1 mW). The sample nucleus plays the role of central conductor shorted at one end to analyze the reflection coefficient S_{11}, from which real R and imaginary X components of impedance are determined.[28] Glass coating was removed from the ends of the microwire to ensure electrical contact to the nucleus. The transmission coaxial line (shown in Fig. 1) was introduced into a solenoid, which supplied a maximum longitudinal DC magnetic field of 48 kA/m, high enough to saturate the wires. Real and imaginary components of impedance were simultaneously measured as a function of the frequency at different applied DC longitudinal fields. In addition, a transversal magnetic field up to 13 kA/m was applied by a pair of Helmholtz coils simultaneously to DC longitudinal field. Before each measurement, all cables, connectors, and adapters were calibrated using short-open-load technique and the electrical delay of coaxial line, 88 ps, was removed. The impedance in the measurement plane was corrected to remove the contribution of the different parts in transmission coaxial line in order to obtain the intrinsic impedance of sample.

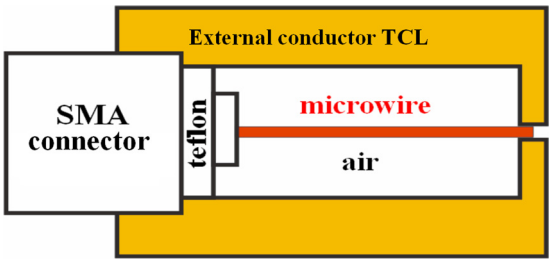

FIG. 1. (Color online) Sketch of the transmission coaxial line (TCL).[25]

III. RESULTS AND DISCUSSIONS

A. Field dependent spectra

Figure 2 shows the complex impedance spectra of real and imaginary components for the as-cast FeCoMoB microwire under zero applied field. This natural ferromagnetic resonance observed in high-magnetostriction alloys is here characterized by four maxima observed at the real part corresponding to four inflection points in the imaginary part indicating their correlation to a resonance effect.[29] The intrinsic magnetic anisotropy plays the saturating role of the lacking applied magnetic field. In fact, complex stress distribution is introduced during the glass-coated microwire production. The magnetoelastic anisotropy arising from the stresses induced during fabrication[30] determines the magnetization easy axis apart from shape anisotropy. It was shown previously in theoretical calculations that three main kinds of internal stresses are quenched-in during the fabrication process: axial, radial, and circular ones[5,31] that define different regions in the radial profile of the wire. In fact, although

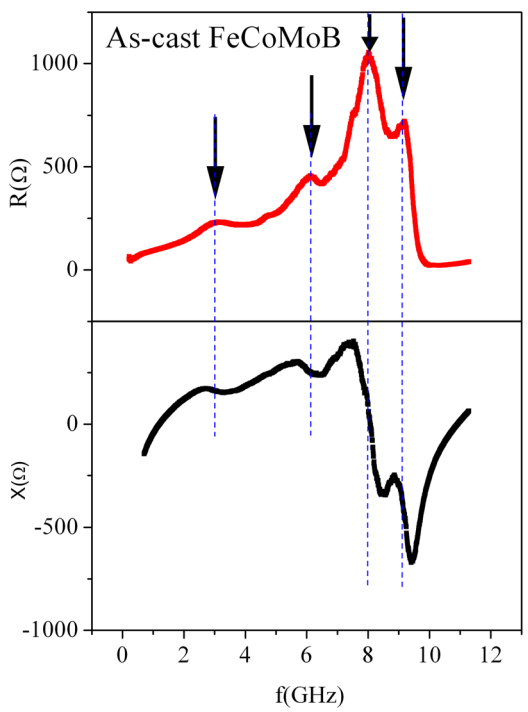

FIG. 2. (Color online) Real (R) and imaginary (X) part of impedance spectra for amorphous as-cast FeCoMoB microwire at zero applied field show multiple peaks as a result of complex stress distribution.

a number of works have been previously devoted to the low-field absorption phenomena in this family of wires[32–34] not much attention has been paid to using FMR as a tool to determine the stress distribution in the microwires.

In order to identify the origin of each absorption phenomenon in Fig. 2, we have studied the FMR under different applied magnetic field. Firstly, we have studied the influence of a magnetic field applied parallel to the longitudinal axis of the wire. As observed in Fig. 3, a relatively small longitudinal field (i.e., 9.6 kA/m) shifts low-frequency maxima toward higher values. Under the application of larger amplitude fields (i.e., 28.8 kA/m), the shift moves to higher frequencies, and simultaneously the number of resonant peaks is reduced to two. For saturating magnetic field (i.e., 48 kA/m), only a single peak is finally observed. On the other hand, we should note that the relative intensity of the peak at around 9 GHz decreases with applied field, but its position is little affected.

The shifting of absorption peaks toward higher frequencies observed with increasing applied field, H_0, just follows Eq. (1). The collapsing of different peaks into finally a single absorption can be understood in terms of competition between applied and local anisotropy fields. When the longitudinal applied field, H_0, exceeds the anisotropy field H_k ($H_0 >> H_k$), in a particular region of the wire that region gets saturated magnetically. Consequently, the absorption corresponding to the original orientation of magnetization is no more observed. Under saturating magnetic field only single peak is detected that corresponds properly to FMR. It was shown in Ref. 4 that radial stresses prevail just under the wire surface, whereas axial stresses are dominant close to the wires center. The FMR measurements are sensitive to the surface of the microwire (due to the small skin depth of the exciting current). In fact, the calculated value of skin depth penetration is much less then 1 μm for all samples and therefore we get only a FMR response from the corresponding surface region of the microwire, where dominant anisotropies are axial and radial. Hence, we can ascribe the last resonance peak (at 9 GHz) to the radial magnetoelastic anisotropy just under the surface and peaks at lower frequency to axial one at more internal region.

B. Thermal treatments and magnetoelastic effects

After annealing at temperatures below 425 °C, the stresses introduced during the microwire's production relax and the structure becomes more homogeneous although, still remaining amorphous.[16] On the other hand, new stresses are introduced by cooling the sample down to room temperature. These additional stresses arise from the difference in thermal expansion coefficient of metallic nucleus and glass coating, and can be expressed as[35]

$$\sigma(T) \approx E(\alpha_g - \alpha_m)\Delta T, \tag{2}$$

where E is the Young's modulus of the metallic core, and α_g and α_m are the corresponding thermal expansion coefficients of the Pyrex and metallic core, respectively.

The resultant impedance spectra of sample annealed at 400 °C displays two well separable peaks at zero applied field (see Fig. 4). As the applied field increases the resonance peaks shift and the intensity of absorption change in a similar way like in as-cast sample. Particularly, the first resonance peak shifts to higher frequencies with increasing applied axial field and its intensity increases steeply. The second peak remains at its position and decreases its intensity. Again, under the saturating applied field (i.e., 48 kA/m) the impedance spectra show a single peak.

Figure 5 shows the very modest influence of transversal applied field on the resonance spectra for the microwire annealed at 400 °C. Only an increase in the relative intensity of the resonance peak at higher frequency is observed since the transversal field affects mainly the transverse magnetoelastic anisotropy. That somehow confirms our idea about the origin of the resonance peak. The axial anisotropy results in the maximum at low frequency and the radial one at the higher frequency. Similarly with our results, Chiriac and coworkers[26] measured two resonance peaks in FMR spectra on FeSiB microwires with high positive magnetostriction. The first resonance peak, located at low frequency, arises from an axial anisotropy and the second one, placed at higher frequency, arises from radial anisotropy.

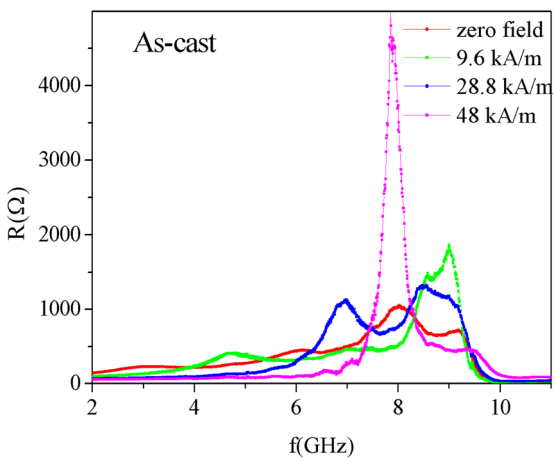

FIG. 3. (Color online) Evolution of resonance spectra (real part of impedance) with DC magnetic field for as-cast sample.

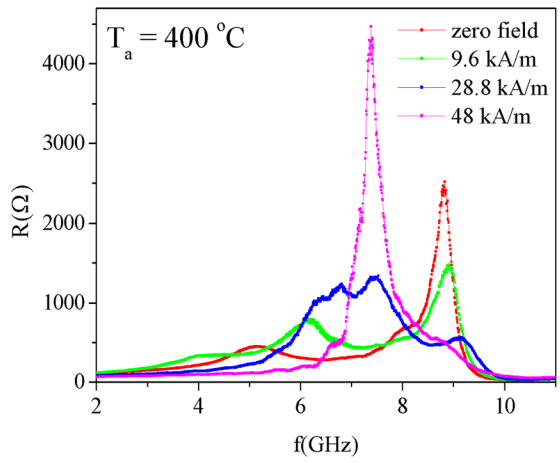

FIG. 4. (Color online) Resonance spectra of real part of impedance for amorphous FeCoMoB microwire annealed at 400 °C: Evolution with axial DC magnetic field.

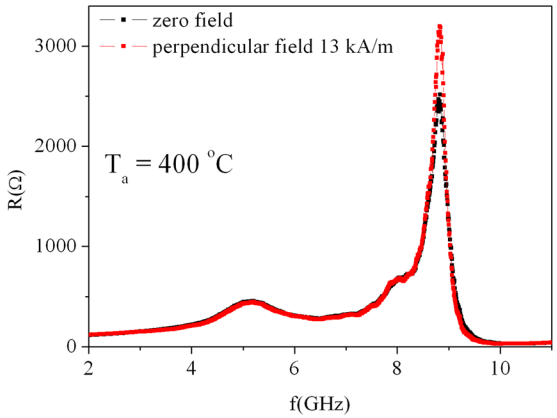

FIG. 5. (Color online) Resonance spectra for amorphous FeCoMoB microwire annealed at 400 °C: The effect of applied transversal field.

Annealing the microwire at temperatures above 425 °C results in its crystallization.[16,36] Firstly, a nanocrystalline structure appears with randomly oriented α-FeCo crystalline grains (size about 12-13 nm) embedded in an amorphous residual phase. Due to the random orientation of easy axis of crystalline grains, together with their small dimensions (lower that exchange length), the effective magnetocrystalline anisotropy vanishes.[37] Moreover, after such treatments a contribution to magnetic anisotropy from magnetoelastic origin should be present due to the positive magnetostriction of both crystalline and amorphous phases.[38] Similarly, the stresses introduced by the glass-coating (by cooling the microwire to room temperature after annealing) together with the magnetoelastic interaction results in the appearance of the axial anisotropy in the center of the wire and radial one just under the surface.

The absorption spectra, after annealing at 450 °C, is shown in Fig. 6. The spectra shows two peaks, much wider than those shown in Fig. 5, obtained after annealing at 400 °C, which reflects a wider distribution of the crystalline grains size and hence the distribution of anisotropies. Application of axial field firstly shifts the first peak position to higher frequencies and finally two peaks are transformed

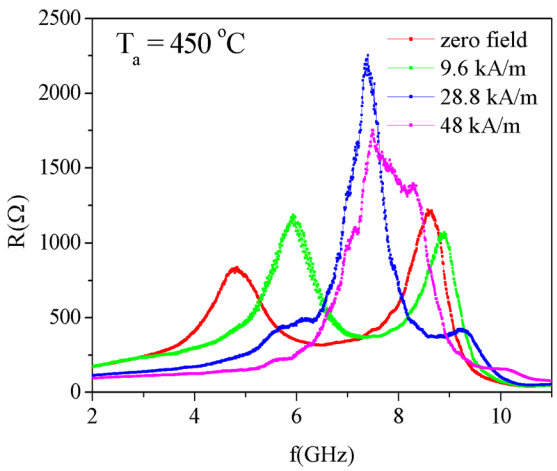

FIG. 6. (Color online) Evolution of real part of impedance spectra with axial DC magnetic field after annealing at 450 °C.

into the single one at highest applied field (48 kA/m). However, the single peak is much more spread in comparison to the one that appears in the microwire annealed at 400 °C. This is assumed to be a result of the anisotropy distribution because of the crystalline grains size and shape distribution in nanocrystalline materials.

Anyway, deeper information can be obtained from the FMR measurements allowing a deeper quantitative analysis of the way. According to Eq. (1), the anisotropy field, H_k can be obtained by extrapolation of the dependence of f_r^2 on H to zero frequency.[39]

Figure 7 shows the dependence of the square resonance frequency of the first peak (at lower frequencies) on the applied axial magnetic field for microwires annealed at various temperatures up to 600 °C for 1 h. The results are divided into two groups corresponding to amorphous (T_a below 400 °C) and nanocrystalline state (T_a above 400 °C). From these dependencies, the anisotropy field H_k can be calculated according to Eq. (1).

The evolution of the anisotropy field H_k with annealing temperature for FeCoMoB microwire is shown in Fig. 8. Strong stresses introduced during the microwire's production result in large magnetoelastic anisotropy at the as-cast state. Annealing below the crystallization temperature leads to stress relaxation and sample homogenization so, indicating that the strong anisotropy field decreases after annealing below 400 °C. Annealing above crystallization temperature (425 °C) has a little effect on the anisotropy field. Such behavior reflects well the switching field dependence on the annealing temperature obtained by induction measurement method from[16] (see inset of Fig. 8). The switching field H_{sw} of closure domain decreases with the temperature of annealing up to 300 °C. Sharp maximum appears at 425 °C as a result of appearance of precipitates of crystalline phase that plays the role of pinning centers for the domain wall propagation.[16,36] Above this temperature, the nanocrystalline structure appears with an exchange interaction between the crystalline grains. Such a structure is very stable and the switching field remains almost constant.

Large internal stresses are induced inside of metal core during production process and these stresses significantly determine the magnetic behavior of the microwire. Both quenching stresses as well as those resulting from the difference between thermal expansion coefficients of metal core and glass cover are present in the microwires. Knowing the anisotropy field H_k (estimated from FMR measurement), it is possible to calculate the internal stresses using the relationship[31]

$$\sigma = \mu_0 M_S H_k / 3\lambda_S \tag{3}$$

for samples after different thermal treatment. The dependence of internal stresses on the annealing temperature is shown in Fig. 9. Although saturation magnetostriction increases with annealing temperature,[40] internal stresses decrease sharply from initial maximum value in the as-cast state. This sample, in its as-cast amorphous state, is characterized by strong internal stresses frozen during the production process. Stress relaxation takes place during annealing process at higher

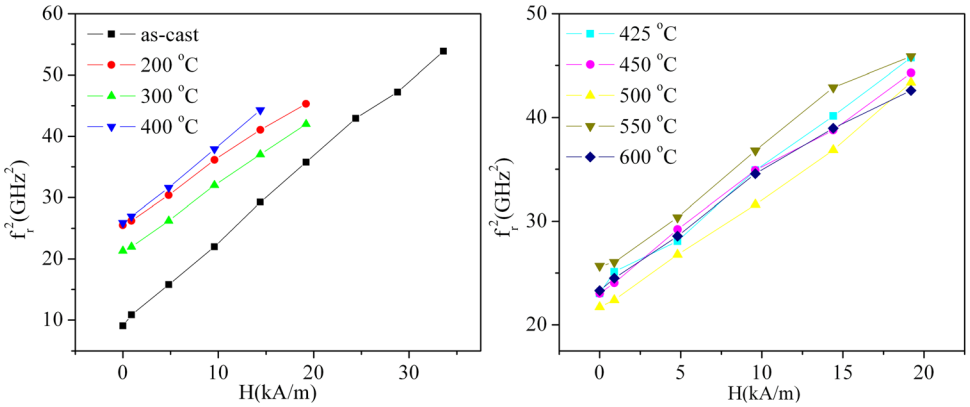

FIG. 7. (Color online) Dependence of the square resonance frequency on the applied axial magnetic field.

temperatures. Therefore, internal stresses quickly decrease in amorphous samples with increasing annealing temperature from maximal value ~800 MPa down to minimal values ~250 MPa in the nanocrystalline state. Finally, microwires in a nanocrystalline state have almost constant and low values of internal stresses. This can explain the results from Ref. 9, where very weak dependence of the switching field was observed on the annealing temperature above 450 °C.

C. Gilbert damping

One of the most important information that can be obtained from FMR measurements are damping parameters. Gilbert damping is the main parameter that influences the domain wall dynamics, and one of the very promising direction of microwire's application is their use in modern spintronic devices based on the domain wall propagation in thin magnetic wires.[9,41,42] Fast domain wall velocity observed in glass-coated microwires is usually ascribed to very low values of Gilbert damping.[43] The Gilbert damping, α, was estimated from measured FMR spectra using the formula[44]

$$\Delta f = (|\gamma|\Delta H_0 + 4\pi\alpha.f)\sqrt{1+\left(\frac{|\gamma|\mu_0 M_S}{4\pi f}\right)^2}, \qquad (4)$$

where Δf is the frequency linewidth, and $|\gamma|\Delta H_0$ is the zero frequency term (that includes all damping terms due to inhomogeneities present in the sample). Figure 10 shows the evolution of measured values of Gilbert damping in the present work range from 0.0127 up to 0.0746. Gilbert damping increases at low annealing temperatures because of stress relaxation takes place, homogenization of sample and stabilization of domain structure. Gilbert damping shows the highest value of 0.0746 above crystallization temperature, exactly at temperature 425 °C. In fact, the structure is changed from amorphous to nanocrystalline at this temperature. The number of crystallites is still low and they are separated by a large distance, that is, the structure is highly nonhomogeneous.[16,36] At higher annealing temperatures, Gilbert damping decreases very shortly down to the lowest value 0.0127. At higher annealing temperatures, the volume fraction of grains is significant[36] and distance between them is smaller than ferromagnetic exchange length ~46 nm.[16] Therefore, exchange interaction between them leads to the averaging out of magnetocrystalline anisotropy, which result in drop of switching field values and as well as Gilbert damping values.[11,16] The obtained values of Gilbert damping correspond well to the ones obtained in glass-coated CoFeSiB microwires[45,46] and its temperature dependence reflects also the temperature dependence of the switching field as described for inset in Fig. 8.

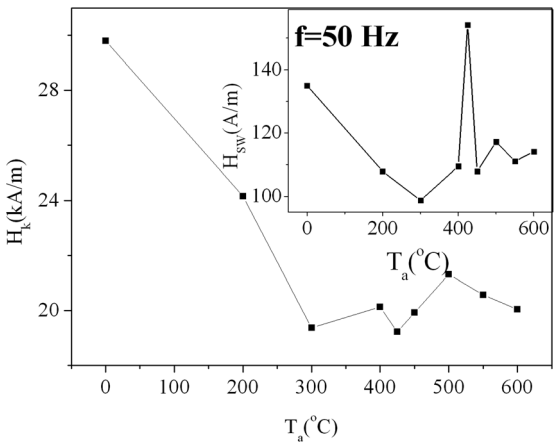

FIG. 8. Evolution of anisotropy field with annealing of the glass-coated FeCoMoB microwire. Inset shows the switching field dependence on the annealing temperature obtained from Ref. 13.

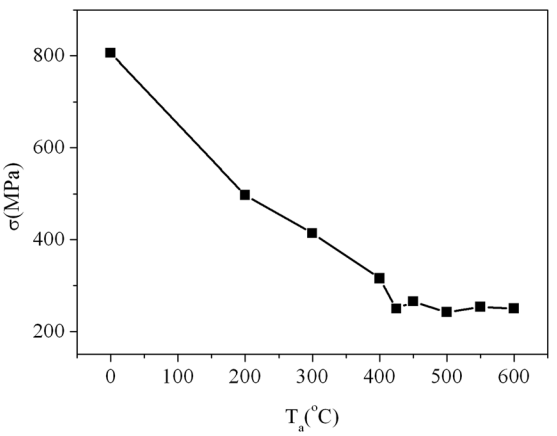

FIG. 9. The dependence of the internal stresses on the annealing temperature.

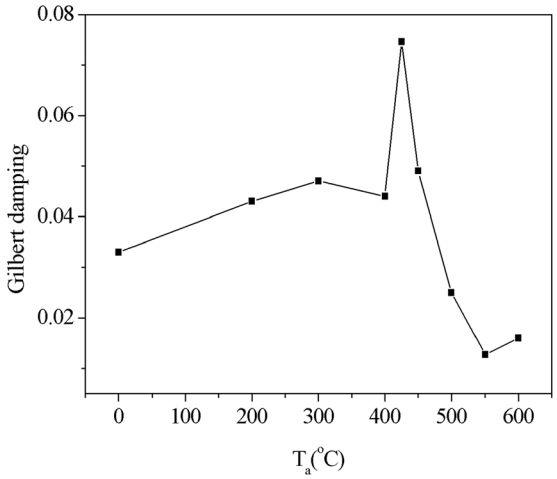

FIG. 10. Dependence of Gilbert damping on the annealing temperature.

IV. CONCLUSIONS

In summary, we have studied the evolution of the microwave absorption phenomena related to ferromagnetic resonance during the devitrification process of the glass-coated FeCoMoB amorphous microwires. A strong natural ferromagnetic resonance was observed in all studied samples. Amorphous sample exhibits a complex impedance spectra with up to four resonance peaks denoting the presence of various regions with different magnetic anisotropy easy axis. During annealing, stress relaxation and homogenization of structure take place and after annealing at the highest temperatures, the microwire displays only two well separable resonance peaks, which correspond to axial and radial domain structure. This effect is significant in both amorphous and nanocrystalline microwires.

Values of anisotropy field and internal stresses have been evaluated from FMR measurements. Anisotropy field decreases with increasing annealing temperature and so does the internal stresses too (they decrease from large values ~800 MPa in initial amorphous sample to low values ~250 MPa in nanocrystalline state). Moreover, internal stresses are low and almost constant in nanocrystalline microwires.

Finally, Gilbert damping which is a relevant parameter determining the domain wall dynamics has very low values and varies from value 0.01 up to 0.05 with exception of the sample annealed at 425 °C. Therefore, these microwires with low damping are very suitable for domain wall dynamics with very fast domain wall propagation.

ACKNOWLEDGMENTS

This work was supported by the project NanoCEXmat Nr. ITMS 26220120019, Slovak VEGA Grant. Nos. 1/0076/09 and APVV-0266-10. P. Klein would like to thank the National Scholarships Programme of the Slovak Republic. It was also partly funded by Spanish MEC under project MAT2007-65420.

[1]M. Vázquez, in *Handbook of Magnetism and Advanced Magnetic Materials*, edited by H. Kronmüller and S. Parkin (Wiley, New York, 2007), Vol. **4**, p. 2193.
[2]A. Zhukov, J. González, M. Vázquez, V. Larin, and A. Torcunov, in *Encyclopedia of Nanoscience and Nanotechnology*, edited by H. S. Nalwa (American Scientific Publishers, Valencia, CA, 2003), Vol. **X**, p. 1.
[3]H. Chiriac and T.-A. Óvári, Prog. Mater. Sci. **40**, 333 (1996).
[4]W. Wulfhekel, H. F. Ding, W. Lutzke, G. Steierl, M. Vázquez, P. Marin, A. Hernando, and J. Kirschner, Appl. Phys. **A72**, 463 (2001).
[5]H. Chiriac, T.-A. Óvári, and G. Pop, Phys. Rev. B **52**, 10104 (1995).
[6]Y. Yoshizawa, K. Yamauchi, T. Yamane, and H. Sugihara, J. Appl. Phys. **64**, 6047 (1988).
[7]M. E. McHenry, M. A. Willard, and D. E. Laughlin, Prog. Mater. Sci. **44**, 291 (1999).
[8]K. Suzuki, N. Ito, J. S. Garitaonandia, and J. D. Cashion, J. Appl. Phys. **99**, 08F114 (2006).
[9]J. Olivera, R. Varga, V. M. Prida, M. L. Sanchez, B. Hernando, and A. Zhukov, Phys. Rev. **B82**, 094414 (2010).
[10]P. Marin, M. Vázquez, A. O. Olofinjana, and H. A. Davies, Nanostruct. Mater. **10**, 299 (1998).
[11]C. Gómez-Polo, A. O. Olofinjana, P. Marin, M. Vázquez, and H. A. Davies, IEEE Trans. Magn. **29**, 2673 (1993).
[12]K. Pekala, J. Latuch, M. Pekala, I. Škorvánek, and P. Jaskiewicz, Nanotechnology **14**, 196 (2003).
[13]J. Arcas, C. Gómez-Polo, A. Zhukov, M. Vázquez, V. Larin, and A. Hernando, Nanostruct. Mater. **7**, 823 (1996).
[14]T.-A. Ovari, H. Chiriac, M. Vázquez, and A. Hernando, IEEE Trans. Magn. **36**, 3445 (2000).
[15]C. Gómez-Polo, P. Marin, L. Pascual, A. Hernando, and M. Vázquez, Phys. Rev. **B65**, 024433 (2002).
[16]P. Klein, R. Varga, P. Vojtanik, J. Kovac, J. Ziman, G. A. Badini-Confalonieri, and M. Vázquez, J. Phys. D: Appl. Phys. **43**, 045002 (2010).
[17]M. Malátek and L. Kraus, Sens. Actuators A: Phys. **164**, 41 (2010).
[18]L. Kraus, M. Vázquez, G. Infante, G. A. Badini-Confalonieri, and J. Torrejon, Appl. Phys. Lett. **94**, 062505 (2009).
[19]D. Ménard, M. Britel, P. Ciureanu, A. Yelon, V. P. Paramonov, A. S. Antonov, P. Rudkowski, and J. O. Strom-Olsen, J. Appl. Phys. **81**, 4032 (1997).
[20]R. Zuberek, M. Gutowski, H. Szymczak, A. Zhukov, and J. Gonzalez, Phys. Status Solidi A **196**, 205 (2003).
[21]R. Zuberek, H. Szymczak, M. Gutowski, A. Zhukov, V. Zhukova, N. A. Usov, K. Garcia, and M. Vázquez, J. Magn. Magn. Mater. **316**, e890 (2007).
[22]M. G. Han, H. P. Lu, and L. J. Deng, Appl. Phys. Lett. **97**(19), 192507 (2010).
[23]H. Chiriac, C. N. Colesniuc, and T.-A. Ovári, J. Magn. Magn. Mater. **215–216**, 407 (2000).
[24]C. Dudek, A.-L. Adenot-Engelvin, and O. Acher, IEEE Trans. Magn. **42**, 2787 (2006).
[25]M. R. Britel, D. Ménard, L. G. Melo, P. Ciureanu, A. Yelon, R. W. Cochrane, M. Rouabhi, and B. Cornut, Appl. Phys. Lett. **77**, 2737 (2000).
[26]H. Chiriac, C. N. Colesniuc, T.-A. Ovári, and F. J. Castano, J. Appl. Phys. **87**, 4816 (2000).
[27]J. M. D. Coey, *Magnetism and Magnetic Materials* (Cambridge, 2010) p. 316.
[28]J. Torrejón, G. A. Badini-Confalonieri, and M. Vázquez, J. Appl. Phys. **106**, 023913 (2009).
[29]S. A. Baranov, Tech. Phys. **43**, 122 (1998).
[30]M. Vázquez, Physica B **299**, 302 (2001).
[31]A. S. Antonov, V. T. Borisov, O. V. Borisov, A. F. Prokoshin, and N. A. Usov, J. Phys. D: Appl. Phys. **33**, 1161 (2000).
[32]M. Vázquez, G. A. Badini-Confalonieri, J. Torrejon, R. Valenzuela, H. Montiel, and G. Alvarez, Third International Conference on Quantum, Nano and Micro Technologies, 134 (2009).
[33]R. Valenzuela, H. Montiel, G. Alvarez, and R. Zamorano, Phys. Status Solidi A **206**, 652 (2009).
[34]H. Chiriac, C. N. Colesniuc, T.-A. Ovari, and M. Ticusan, J. Appl. Phys. **85**, 5453 (1999).
[35]R. Varga, K. L. Garcia, A. Zhukov, M. Vazquez, and P. Vojtanik, Appl. Phys. Lett. **83**, 2620 (2003).
[36]S. Michalik, J. Gamcova, J. Bednarčík, and R. Varga, J. Alloys and Compounds **509**, 3409 (2011).
[37]G. Herzer, J. Magn. Magn. Mater. **294**, 99 (2005).
[38]K. Suzuki, K. N. Ito, J. S. Garitaonandia, J. D. Cashion, and G. Herzer, J. Non-Cryst. Solids **354**, 5089 (2008).
[39]C. Kittel, *Introduction to Solid State Physics* (Wiley, New York, 1996), Ch. 16, p. 503.
[40]G. Vlasák, M. Pavúk, P. Mrafko, D. Janičkovič, P. Švec, and B. Butvinová, J. Magn. Magn. Mater. **320**, e837 (2008).

[41]R. Varga, A. Zhukov, V. Zhukova, J. M. Blanco, and J. Gonzalez, Phys. Rev. B **76**, 132406 (2007).
[42]R. Varga, K. L. Garcia, M. Vázquez, and P. Vojtanik, Phys. Rev. Lett. **94**, 017201 (2005).
[43]D. Atkinson, D. A. Allwood, G. Xiong, M. D. Cooke, C. C. Faulkner, and R. P. Cowburn, Nature Mater. **2**, 85 (2003).
[44]S. S. Kalarickal, P. Krivosik, M. Wu, C. E. Patton, M. L. Schneider, P. Kabos, T. J. Silva, and J. P. Nibarger, J. Appl Phys. **99**, 093909 (2006).
[45]K. D. Sossmeier, F. Beck, H. Chiriac, L. F. Schelp, and M. Carara, Phys. Stat. Sol. A **206**, 635 (2009).
[46]M. Ipatov, V. Zhukova, A. Zhukov, J. Gonzalez, and A. Zvezdin, Phys. Rev. **B 81**, 134421 (2010).